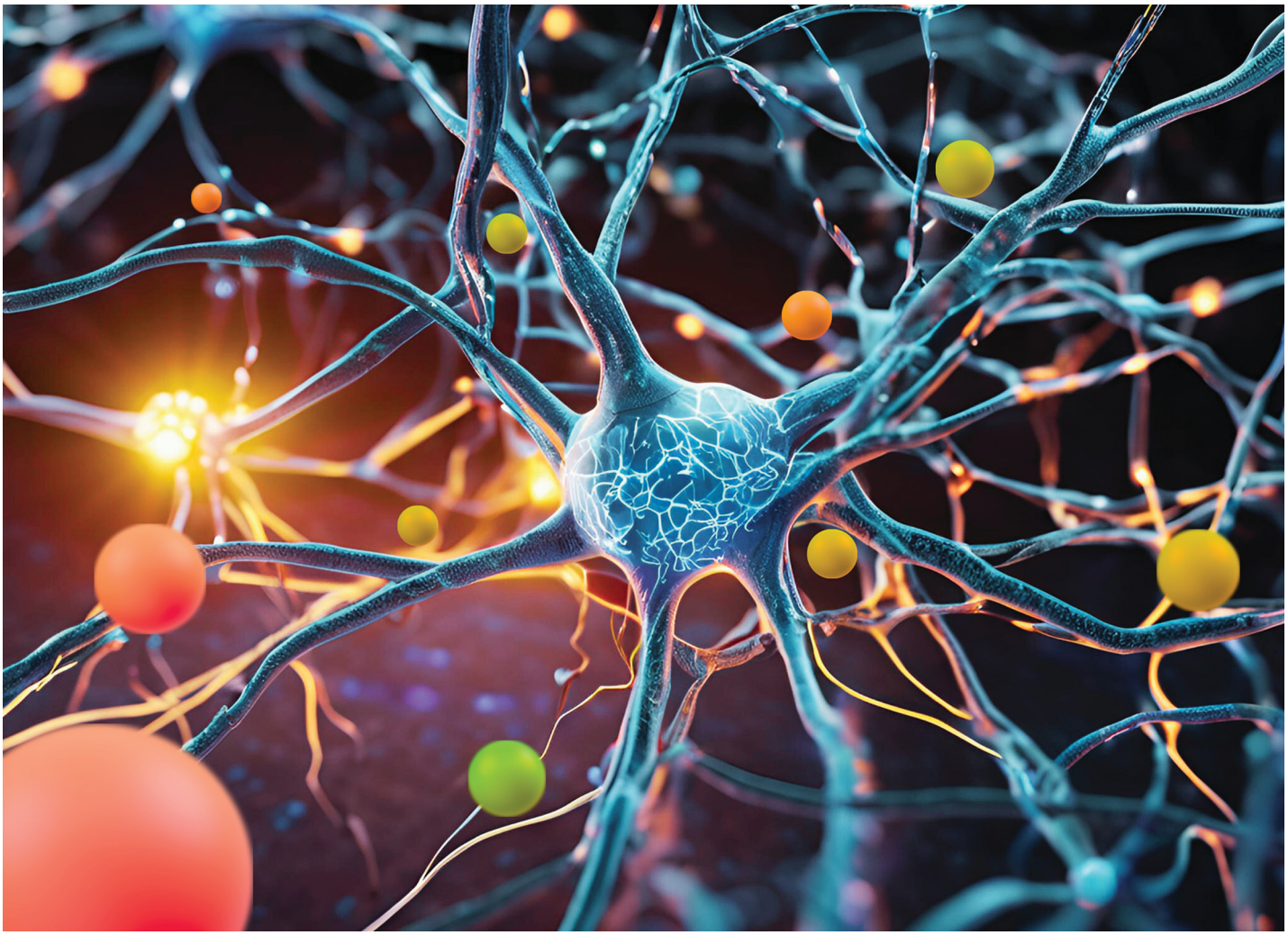

Showcasing research from Dr del Mercato's laboratory, Nanotechnology Institute of National Research Council (CNR-NANOTEC), Lecce, Italy.

A fluorescent ratiometric potassium sensor based on IPG4-silica microparticles for selective detection and fluorescence imaging of potassium cations

We developed a biocompatible fluorescent microsensor for potassium (K^+) detection, using ION potassium green 4 as the probe and silica as the core material. Optimized for fluorescence imaging, it enables non-invasive ratiometric optical detection and monitoring of K^+ fluctuations in biological systems. These high-precision tools provide valuable insights into potassium's role in cellular processes like neurotransmission and muscle contraction.

As featured in:

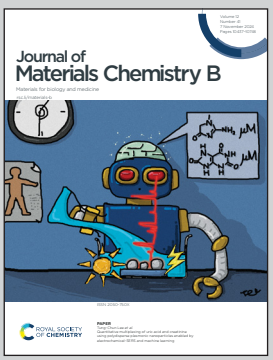

See Loretta L. del Mercato *et al.*, *J. Mater. Chem. B*, 2024, **12**, 10573.

ROYAL SOCIETY OF CHEMISTRY

rsc.li/materials-b

Registered charity number: 207890

Journal of Materials Chemistry B

ROYAL SOCIETY OF CHEMISTRY

PAPER

View Article Online
View Journal | View Issue

Check for updates

Cite this: J. Mater. Chem. B, 2024, 12, 10573

A fluorescent ratiometric potassium sensor based on IPG4-silica microparticles for selective detection and fluorescence imaging of potassium cations†

Francesco Colella, [ab] Stefania Forciniti, [a] Valentina Onesto, [a] Giuliana Grasso, [a] Helena Iuele, [a] Giuseppe Gigli[ac] and Loretta L. del Mercato *[a]

Received 14th May 2024,
Accepted 19th August 2024

DOI: 10.1039/d4tb01047g

rsc.li/materials-b

Potassium cations play many important roles in living organisms, especially in electro-physiology, since they are involved in neurotransmission and muscle contractions. We report the synthesis of a ratiometric fluorescent microsensor for potassium (K^+) detection, based on the fluorescent probe ION potassium green 4. Potassium-sensitive fluorescent microparticles were obtained by using silica as the core material. We obtained silica-based microsensors with sizes in the micrometer range, spherical shapes, good monodispersity, optimal selectivity and a sensitivity range of 0 to 40 mM. The microsensors also proved to be non-toxic in cell cultures and suitable for fluorescence imaging, offering new possibilities for non-invasive optical detection, quantification and *in situ* monitoring of K^+ variations in cell culture systems.

Introduction

Potassium cations (K^+) are among the most important inorganic ions for electro-physiological processes, being essential for both muscle contraction and neuron communication.[1] To maintain cell membrane potentials, the K^+ ion concentration in plasma and interstitial fluids should be almost 100 times smaller compared to the intracellular one (extracellular 3–5 mM and intracellular 100–150 mM).[1] Such a concentration difference is essential for animal physiology and is kept constant by the activity of the Na^+/K^+ ATPase pump and kidney filtration.[1] Dysregulation in K^+ homeostasis is involved in pathophysiological events, mainly cardiac (*i.e.* cardiac arrhythmia) and central nervous system dysfunctions (*i.e.* migraine and epilepsy).[1–3] There is also evidence that K^+ ion accumulation plays a relevant role in cancer, by creating a hostile environment for immune cells, preventing them from attacking the tumors.[4,5] Considering that dysregulation of K^+ concentration is involved in different pathological phenomena, the development of new tools for precisely studying and detecting their variations in *in vitro* and *in vivo* models is still a hot topic. Among the most common techniques for measuring cation variation in biological systems, ion-selective electrodes (ISEs) and microelectrode arrays (MEAs) are largely used for sensing ion concentrations, including K^+. Nonetheless, they have limitations related to cation selectivity,[6] low sensitivity, potential interference from other ions, circumscribed spatial resolution (*e.g.*, only K^+ concentrations in close proximity to the electrode can be detected), limited measurement duration and complexity of data interpretation.[7] An alternative approach to electrochemical sensors is ion-selective optodes (ISOs), which are the optical equivalent of an electrode, usually based on optical fibers.[8,9] Meanwhile, the patch clamp technique is largely used to measure ion fluxes through cell membranes in biological samples.[10,11] Optical methods for cation analyses are based on fluorescent organic probes, which are able to bind cations and give a quantitative response resulting from a fluorescence enhancement or quenching of the emission intensity.[12–16] However, the selectivity between different cations is an issue even in this case.[14] New molecular approaches (*i.e.*, probes and fast-responding chemo- and nanosensors) are currently under development. These fluorescent probes can be ratiometric or non-ratiometric. In a ratiometric sensor, the final readout is given by the ratio of the sensitive signal and a non-sensitive signal. Furthermore, a molecular probe can be intrinsically ratiometric, with two fluorescence emission signals, one of which is insensitive to the analyte. In the case of non-ratiometric probes, a second fluorescent dye can be used as a reference signal.[15–18] In the last few years several

[a] Institute of Nanotechnology, National Research Council (CNR-NANOTEC), c/o Campus Ecotekne, via Monteroni, 73100, Lecce, Italy. E-mail: loretta.delmercato@nanotec.cnr.it
[b] Department of Mathematics and Physics "Ennio De Giorgi", University of Salento, c/o Campus Ecotekne, via Monteroni, 73100, Lecce, Italy
[c] Department of Experimental Medicine, University of Salento, c/o Campus Ecotekne, via Montero-ni, 73100, Lecce, Italy

† Electronic supplementary information (ESI) available. See DOI: https://doi.org/10.1039/d4tb01047g

prototypes of K^+ sensing micro/nanoparticles were reported. One of the approaches more similar to the one we adopted in this study was reported by MacGilvary *et al.*, which utilized bovine serum albumin (BSA)-coated silica microparticles to covalently bind IPG4 (ION Potassium Green 4, ION Biosciences, United States) as a sensitive dye and Alexa Fluor 594 as a reference dye. The result was a ratiometric microsensor with a sensitivity for K^+ concentration from 0 to 128 mM.[19] Xie, Xiaojiang *et al.* reported the synthesis of fluorescent K^+-sensitive polystyrene microparticles. However, despite these microsensors showing good selectivity towards K^+ over Na^+, Li^+ and bivalent cations (Ca^{2+} and Mg^{2+}), the sensitivity range of the microsensors is from 0 to 60 μM, which is too low for monitoring [K^+] in biological samples.[20] Lee Chang H. *et al.* reported the synthesis of dual-mode K^+-sensing nanoparticles that can be used as fluorescent ratiometric sensors or for photoacoustic imaging. These nanosensors displayed a sensitivity from 1 mM to 1 M, which could be suitable for monitoring both intracellular and extracellular K^+ variations. However, the system showed interference with other cations, especially Na^+.[21] One of the most commonly used molecular probes for measuring K^+ concentration changes in living cells is potassium-binding benzofuran isophthalate (PBFI),[22–25] which has major limitations. PBFI has limited specificity: it is only 1.5-fold more selective toward K^+ compared to sodium cations (Na^+), which makes it more suitable for intracellular sensing (where the Na^+ concentration is only 5–30 mM), displays weak fluorescence, and is difficult to load intracellularly.[26] The other limitation is that PBFI needs to be excited in the far UV region, with a laser source of 350 nm, which might have harmful effects on living cells.[27]

In this study, we developed a stable and highly sensitive optical sensor for K^+ detection. To overcome the limitations of the current sensors, we chose Asante potassium green 4 (APG-4), recently renamed ION Potassium Green 4 (IPG4) (ION Biosciences, United States), which is reported to be the most selective, currently available, fluorescent probe for K^+, since it is declared to be 100 times more selective toward K^+ compared to Na^+. The manufacturer declares a sensitivity range of 0–38 mM with a saturation kinetic and a K_d of 7 mM.[28] The IPG4 fluorescence emission displays an increase correlated with the increase in K^+ concentration. The fluorescence emission is in the green region of visible light, and the declared λ_{ex} max is at 525 nm, although it can also be excited with a 488 nm laser line. We then characterized the physicochemical properties of the sensor, assessed its biocompatibility and application in a cell culture system, and proposed a fluorescent ratiometric microsensor for applications in high-resolution imaging of biological models, allowing real-time monitoring of K^+ variations.

Experimental section

Synthesis of the microsensors

A solution composed of 60 mL of EtOH, 7 mL of MilliQ water, 9 mL of NH_4OH 28%, and 15 mg of KCl was poured into a 250 mL reaction flask, sealed with a rubber septum and kept under stirring at 250 rpm. A solution composed of 35 mL of anhydrous ethanol and 2.38 mL of TEOS was injected into the reaction flask by using a syringe pump, with a flow rate of 0.12 mL min^{-1}. After injection, the reaction mixture was kept under stirring for 12 hours at 250 rpm at room temperature.

The obtained silica microparticles were purified by centrifugation at 2500 rpm for 5 minutes at 21 °C. The pellet was suspended in 50 mL of ethanol and centrifuged again at 2500 rpm for 5 minutes at 21 °C. The washing steps were repeated 3 times.

For the synthesis of aminated microparticles, 500 mg of the obtained silica microparticle core were suspended in 30 mL of anhydrous ethanol and sonicated in a sonication bath for 10 minutes. The microparticle suspension was poured into a 100 mL reaction flask and sealed with a rubber septum. A solution composed of 10 mL anhydrous ethanol, 250 μL TEOS and 50 μL APTES was injected into the reaction flask through a syringe pump at a flow rate of 0.05 mL min^{-1}. The reaction mixture was kept under stirring at 300 rpm, at RT, for 12 hours. The aminated microparticles were then washed by centrifugation 3 times (2500 rpm, 5 minutes, 21 °C). The ninhydrin assay was used to check for successful aminosilanization on the plain microparticle surface (see the Ninhydrin assay section).

SiO_2@IPG4 MPs were obtained by amide coupling with HATU. 100 mg of SiO_2@NH_2 were suspended in DMF and centrifuged 3 times at 8000 rpm for 4 minutes on a benchtop centrifuge in order to remove residual ethanol and water. The microparticles were then suspended in 1 mL of DMF. IPG4 lyophilized powder was solubilized in DMF, and the corresponding volume of 50 μg of IPG4 was diluted in 100 μL of DMF. HATU was solubilized in DMF at a known concentration, and the corresponding volume for 1.9 molar equivalents (26.6 μg) was added to the IPG4 solution. 10 μL of DIPEA were added as the base catalyst to the solution, and the solution was kept in the dark for 30 minutes (in order to obtain complete activation of the carboxylic functions). Activated IPG4 solution was added to the silica MP suspension, DMF was added to a final reaction volume of 2 mL, and the reaction was kept under stirring for 1 hour. The resulting microparticles were then washed 3 times by centrifugation in ethanol (2500 rpm, 5 minutes, 21 °C).

SiO_2@RBITC-IPG4 MPs were obtained by forming an outer shell of RBITC around silica using a slightly different protocol. 6 mg of RBITC were dissolved in 2 mL of DMF, and 50 μL of APTES was added to the solution. The reaction mixture was kept under stirring for 3 hours (600 rpm, RT). 500 mg of the silica microparticle core were suspended in 30 mL of ethanol and sonicated in a sonication bath for 10 minutes. The microparticle suspension was poured into a 100 mL reaction flask and sealed with a rubber septum. 8 mL of anhydrous ethanol, 250 μL of TEOS and 50 μL of APTES were added to the previous solution containing RBITC-APTES. The solution was injected into the reaction flask through a syringe pump at a flow rate of 0.05 mL min^{-1}. The reaction mixture was kept under stirring at 300 rpm, at RT, for 12 hours. The microparticles were then washed by centrifugation 3 times (2500 rpm, 5 minutes, 21 °C). The ninhydrin assay was used to check if the microparticles were aminated (see the Ninhydrin assay section). The last step

for the conjugation of IPG4 to obtain SiO_2@RBITC-IPG4 was the same as that previously described for the synthesis of SiO_2@IPG4.

The same protocol for the synthesis of SiO_2@RBITC-IPG4 was also used for the synthesis of SiO_2@Cy3-IPG4 by switching RBITC with Cy3.

Ninhydrin assay

2 mg of dry silica microparticles were suspended in 1 mL of ethanol in a 1.5 mL plastic tube. 100 μL of ninhydrin solution (2% w/v in ethanol) were added to the solution. The plastic tubes were placed in a thermoshaker and allowed to react for 20 minutes at 90 °C and 200 rpm. The tubes were cooled down in an ice-cold bath and then centrifuged at 8000 rpm for 5 minutes. The supernatant was collected, and the absorbance at 570 nm was measured using a CLARIOstar Plus plate reader (BMG LABTECH, Ortenberg, Germany). A solution without microparticles was used as a negative control, and five glycine solutions of known concentrations were used to plot the calibration curve.

Physical characterization

The size and morphology of the microsensors were characterized by scanning electron microscopy (SEM, Sigma 300VP, Zeiss, Germany; accelerating voltage of 5 kV, secondary electron detector (SE2), 5000×, 10000× and 30000× magnification). All the samples were sputter-coated (compact coating unit CCU-010, SafeMatic GmbH, Zizers, Switzerland) with a 10 nm-thick gold layer (Target Au Ø 54 mm × 0.2 mm; purity, 99.99%) prior to their observation under a microscope. The mean diameter of the microparticles was obtained with Fiji Imagej (**https://imagej.net/software/fiji/.net**, NIH, USA) based on the SEM diameter of 100 microparticles.

The hydrodynamic diameter and surface charge of the microparticles were assessed by dynamic light scattering (DLS) and zeta potential (ZP) analysis using a Zetasizer Nano ZS90 (Malvern Instruments, Malvern, Worcestershire, UK) equipped with a 4.0-mW He–Ne laser operating at 633 nm, while an avalanche photodiode detector was used. A semi-microcuvette (BRAND®, PMMA, minimum filling volume 1.5 mL, #BR759115) was used for the DLS analysis. A disposable folded capillary ζ cell (Malvern Instruments, Malvern, Worcestershire, UK; #DTS1070) was used for loading the sample. Deionized water was used as the dispersant (n = 1.33 and η = 0.88), and the measurements were performed at 25 °C. The refractive index used during the acquisitions was taken as n = 1.54 and the absorption as k = 0.00. The microsensor stock solutions (40 mg mL^{-1}) were diluted in ultrapure water by pouring 10 μL of the stock solution in 1 mL of MilliQ water. The suspensions were vortexed and then sonicated in a sonication bath for 10 minutes at 40 kHz.

Calibration and stability evaluation of the microsensors

The fluorometric calibrations of the IPG4 dye, the IPG4 conjugated silica microparticles, and different prototypes of the ratiometric microsensors were all performed in [K^+] adjusted MES buffer (50 mM, pH 7.5) in the spectral scan mode using a CLARIOstar Plus plate reader (BMG LABTECH, Ortenberg, Germany). All experiments were performed in black 96-well plates (Corning® 96-well Black Flat Bottom Polystyrene NBS Microplate, Corning, Glendale, Arizona, USA; #3650). To evaluate the stability of the sensing probes, ratiometric fluorescent microparticles (2 μL, stock solution 40 mg mL^{-1}) were incubated with different concentrations of K^+ (0, 10 mM, 20 mM, and 40 mM) in MES buffer. The microplate was stored in the dark at 4 °C for 7 days. Fluorescence readout was monitored and collected on days 1, 3, 5 and 7. K^+ detection was obtained *via* ratiometric calculations obtained by emission peak integration. The fluorescence spectra of the microsensors were extracted as follows: for IPG4, λ_{ex} = 488 nm and λ_{em} = 510–570 nm; and for RBITC, λ_{ex} = 555 nm and λ_{em} = 570–700 nm.

The CLSM-based calibration of the microsensors was performed using a ZEISS LSM-700 (Carl Zeiss, Jena, Germany) by dispersing the K^+ sensitive microparticles in [K^+] adjusted MES buffer (50 mM, pH 7.5). Samples were immobilized on a μ-Slide 8 Well Ibidi® chamber plate (Ibidi GmbH, Gräfelfing, Germany, #80827), previously functionalized with poly-lysine (0.3% in water). Micrographs were acquired using a PlanApochromatic 63X/1.4 oil DIC objective (213.39 μm × 213.39 μm) and a resolution of 1024 × 1024 pixels. A 488 nm argon laser line and a 555 nm laser line were used as excitation sources.

Image analysis

CLSM images were analysed using a previously developed algorithm[12,13] for the automatic segmentation and extraction of the fluorescence intensities experienced by single microparticles. Briefly, reference channel images were pre-processed and binarized to remove noise in the images, small holes in the objects, and suppressing structures that were connected to the image border. Then, the images were segmented by a watershed transformation[29] to identify single particles in the binarized reference channel. This image was used as a mask to extract the pixel-by-pixel ratio of the fluorescence intensities between the indicator and reference channels for each microparticle. Finally, the mean and standard deviation of all considered sensors were determined.

Biocompatibility evaluation

The cytotoxicity of SiO_2@RBITC-IPG4 microparticles was evaluated using the CellTiter-Glo® Cell Viability Assay (Promega Corporation, Germany) on breast cancer cells MCF-7 (HTB-22™; ATCC, Rockville, USA), human pancreatic cancer cells PANC-1 (CRL-1469™; ATCC, Rockville, USA), melanoma cell line SKMEL-2 (HTB-68™; ATCC, Rockville, MD, USA), and 3T3 murine fibroblasts (CCL-163™; ATCC, Rockville, USA) cultured at 37 °C in a humidified 5% CO_2 incubator. SK-MEL-2 cells were cultured in Eagle's minimum essential medium (MEM, Sigma-Merck KGaA, Darmstadt, Germany), whereas Panc-1, MCF-7 and 3T3 fibroblasts were grown in Dulbecco's modified Eagle's medium (DMEM; Sigma-Merck KGaA, Darmstadt, Germany), supplemented with 10% fetal bovine serum (FBS; Gibco, Thermo Fisher Scientific Inc., Waltham, MA, USA), 2 mM L-glutamine, and 100 U mL^{-1} penicillin and streptomycin (Sigma-Merck KGaA, Darmstadt, Germany). Cells (5×10^3 cells per well) were seeded in 96-well plates and treated with or

without K^+ sensing microparticles at final concentrations of 0.05, 0.1 and 0.3 mg mL^{-1}. Cell viability based on the quantification of ATP produced by metabolically active cells was measured at 0, 24 and 48 hours by adding CellTiter-Glo® reagent equal to the volume of the medium present in each well. Then, the samples were mixed for 5 minutes to induce cell lysis and allow the extraction of ATP from live cells. Subsequently, the samples were incubated for an additional 25 minutes at room temperature to equilibrate the luminescence signal. Luminescence was recorded using a CLARIOstar Plus plate reader (BMG LABTECH, Ortenberg, Germany). The viability of untreated cells was used as a control, and the luminescence values of the medium containing the sensors were subtracted from those of the treated or untreated samples.

Evaluation of microsensor properties in cell cultures

SK-MEL2 tumor cells were counted by trypan blue dye exclusion, and 6×10^4 cells per well were seeded into a μ-Slide 4 Well (Ibidi® GmbH, Gräfelfing, Germany). After 24 hours, the cells were stained with the nuclear marker, Hoechst 33342 (B2261, Sigma Aldrich), for 20 minutes, washed in PBS 1× and treated with K^+ sensing microparticles at a final concentration of 0.05 mg ml^{-1}. Then, cells were stimulated with 1 μM nigericin for 1 hour at 37 °C in order to induce K^+ efflux by forming pores on the plasma membrane. Untreated cells were used as controls. Representative images were acquired using CLSM (LSM 980, ZEISS, Germany) equipped with a 40× oil-immersion objective. The maximum projections of the *z*-stack images were obtained using Image J software. For fluorometric measurements of K^+ concentration in the cell culture media, SKMEL-2 cells (5×10^3 cells per well) were seeded in 96-well plates and treated with or without 1 μM nigericin for 1 hour. Then, the cell culture supernatant was collected for each condition and K^+ sensing microparticles were added at a final concentration of 0.5 mg ml^{-1}. Samples were analyzed in a black 96-multiwell plate using a CLARIOstar plate reader (BMG Labtech, Ortenberg, Germany) in the spectral scan mode.

Statistical analysis

The experiments were performed in triplicate, and the results are reported as the mean ± standard error unless otherwise stated. The limit of detection (LOD) was calculated as $LOD = 3\sigma/s$, where σ is the standard deviation of blank measurements (without K^+) and s is the slope of the ratio *versus* K^+ concentration. Statistical differences were considered significant at $p < 0.05$ using a two-way analysis of variance.

Results

Design and synthesis of fluorescent ratiometric microsensors

In order to design a fluorescent ratiometric K^+ microsensor, two fluorescence signals are required: one that must be analyte-sensitive and the second that must be non-sensitive to the analyte. Some organic fluorescent probes are intrinsically ratiometric (*e.g.*, pyranine as a pH-sensitive probe[17,30]), but IPG4 is a non-ratiometric probe for K^+ detection. Therefore, we must supply the microparticles with a second fluorescence signal, which will provide an inner reference signal. We selected different fluorescent dyes to be used in combination with IPG4. The main requirement for the reference dye was fluorescence emission in a different region of visible spectra, avoiding any overlap with the emission peak of IPG4. Based on known spectral properties, we used different fluorophores as potential candidates (as listed in Table S1, ESI†). We synthesized silica particles as the starting material for the proposed ratiometric microsensors due to their inertness and customizable chemical properties.[31] Silica microparticles were produced using a modified Stöber reaction by exploiting TEOS hydrolysis in an alkaline hydroalcoholic solution.[32,33] This method allowed the reproducible and scalable production of silica microparticles with their fine control over size and shape by tuning the reaction conditions.[17,32] The obtained silica microparticles (with a size of approximately 1.5 + 0.4 μm; see Fig. 3 and Table 1) were silanized using APTES in anhydrous ethanol. The presence of free primary amines on the surface of the microparticles (due to APTES silanization) was confirmed and quantified using a ninhydrin colorimetric assay (see Table S2 and Fig. S1, ESI†).

The next step was the conjugation of IPG4 onto the aminated silica microparticles. IPG4 TMA salt was used for functionalization by exploiting the two carboxylic groups, which characterize the molecular structure of the probe to obtain an amide bond on the microparticle surface (see Fig. 1a). All attempts of using EDC as a coupling agent produced no results. Therefore, we performed amide synthesis using HATU as the coupling agent and DIPEA in DMF as the solvent (see Fig. 1d). Following the IPG4 immobilization step, the microparticles displayed a bright pink color, indicating binding of the probe to the SiO_2 microparticles.

The correct conjugation of IPG4 on the silica surface was further confirmed by fluorometric calibration and kinetic calibration (see the optical and kinetic characterization section).

The next step in the synthesis of ratiometric microsensors is the immobilization of the two fluorophores on the silica surface. The strategy that we adopted was based on the formation of an outer shell of the reference dye on the surface of the microparticle, with an excess of APTES that should supply the free primary amino groups for the further conjugation of IPG4 (see Fig. 1e). All of the selected dyes, listed in Table S1 (ESI†), were used in this way to produce a ratiometric system. Only two of the selected reference dyes showed the correct properties for integration in the ratiometric scheme, which were RBITC and Cy3 (the molecular structures of the molecules are shown in Fig. 1b and c). However, all these molecules showed the FRET

Table 1 DLS analyses of the obtained microsensors

	Diameter (μm)	PDI	ζ-potential (mV)
SiO_2@IPG4	1.66 ± 0.11	0.333	−9.41 ± 0.97
SiO_2@Cy3-IPG4	1.57 ± 0.05	0.230	−1.26 ± 0.67
SiO_2@RBITC-IPG4	1.96 ± 0.16	0.338	−10.2 ± 0.68

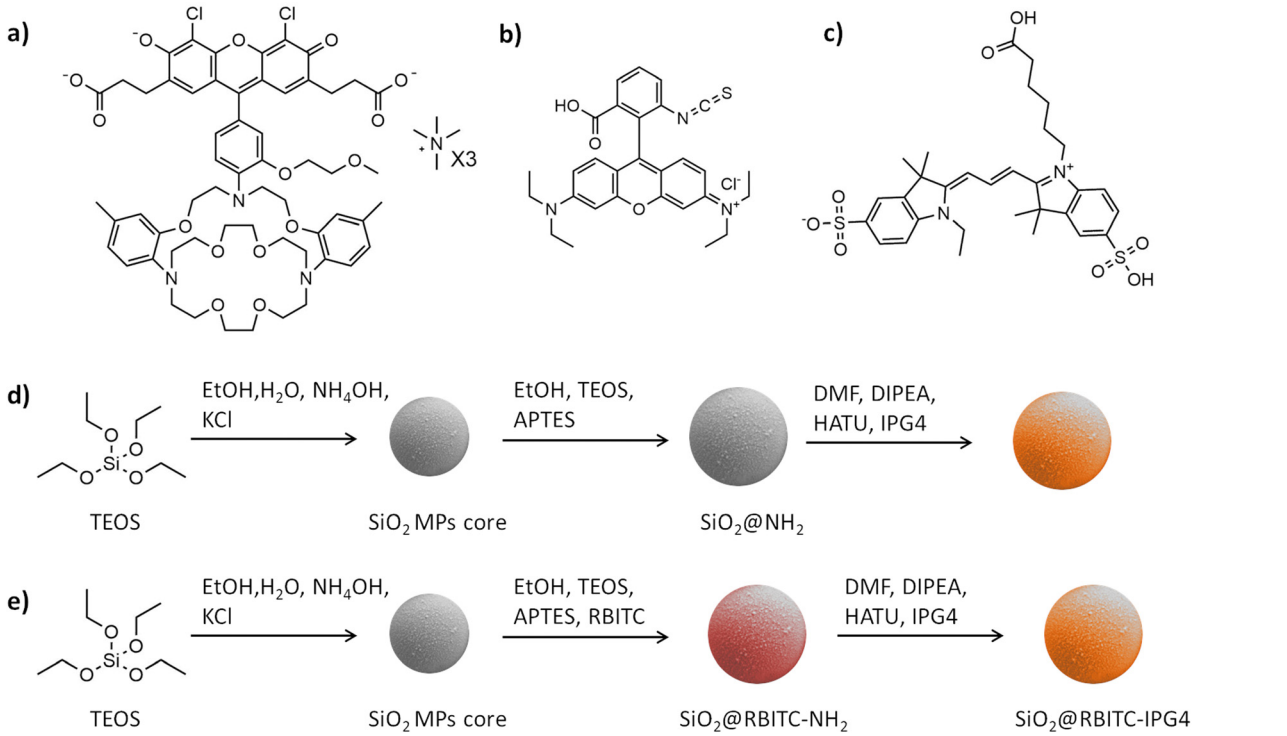

Fig. 1 Molecular structure of the employed dye and synthetic scheme for the synthesis of silica microsensors: (a) molecular structure of IPG4 TMA salt; (b) molecular structure of rhodamine B isothiocyanate; (c) molecular structure of cyanine 3; (d) synthesis scheme with reaction conditions of SiO_2@IPG4; and (e) synthesis scheme with reaction conditions of SiO_2@RBITC-IPG4.

phenomenon with IPG4 when immobilized on the surface of silica microparticles (see Table S1, ESI†).

Optical and kinetic characterization

In order to evaluate the successful binding of IPG4 on the surface of the silica microparticles and their selectivity towards K^+ ions, the optical properties of the IPG4 probe and IPG4-conjugated silica microbeads were analyzed. The emission spectra of IPG4 with different concentrations of K^+ (using KCl dissolved in MES buffer) and with different concentrations of Na^+ (using NaCl dissolved in MES buffer) were recorded at two excitation wavelengths (488 nm and 525 nm). Based on the physiological range of concentrations of Na^+ and K^+ in the interstitial fluids, relatively 100–150 mM for Na^+ and 3–5 mM for K^+, the sensitivity of IPG4 in the cation concentration range from 0 to 150 mM was explored.

As shown in Fig. 2a and b, the IPG4 dye displayed sensitivity only for K^+ with no sensitivity toward Na^+ in the 0–150 mM range. Notably, the same sensitivity was retained following immobilization of the fluorescent probe on the silica microparticles (see Fig. 2d and e), likely indicating that the immobilization steps did not affect the properties of the IPG4 probe.

The dissociation constant (K_d) and maximum specific binding (B_{max}) of K^+ and Na^+ were calculated for both IPG4 and IPG4 conjugated to silica microparticles. As reported in Table S3 (ESI†), the calculated K_d for K^+ may vary based on the excitation wavelength and sensing platform (K_d = 7 mM, ION Biosciences), while B_{max} was comparable in all systems (~105 mM). All the sensing systems, with both excitation wavelengths, showed a low binding capacity for sodium cations (Na^+) (Fig. 2), with a B_{max} of approximately 20 mM. Furthermore, there were no major differences in the results obtained with λ_{ex} 488 nm and λ_{ex} 525 nm (Fig. 2 and Table S3, ESI†), proving that the IPG4 probe was suitable for K^+ mapping using a 488 nm argon laser line exploited in confocal laser scanning microscopy (CLSM).

The calibration curves were obtained for the different prototypes of ratiometric microsensors. However, only two prototypes showed appropriate optical properties for the ratiometric system, namely SiO_2@RBITC-IPG4 and SiO_2@Cy3-IPG4. All of the prototypes showed a FRET phenomenon between the dyes due to their proximity to the silica surface. Among the selected dyes, 7ACC1 exhibited maximum fluorescence emission before λ_{ex} max of IPG4. However, 7ACC1 displayed a different λ_{em} max when covalently bound to silica, with an emission shift to lower wavelengths, between 500 and 600 nm (see Fig. S2, ESI†), overlapping with the fluorescence emission of IPG4. We hypothesized that the red-shift of the spectra could be related to the conversion of the free carboxylic acid to amide. Hence, microparticles defined as SiO_2@IPG4-7ACC1 were not suitable as ratiometric K^+ microsensors.

The emission spectrum of SiO_2@A594-IPG4 also showed an obvious FRET[34] phenomenon. Indeed, the emission peak of A594 was the only one detectable after the conjugation of both fluorophores on silica microparticles at three different excitation wavelengths (488 nm, 525 nm and 555 nm). Unexpectedly, SiO_2@A594-IPG4 showed an inverted correlation to increasing

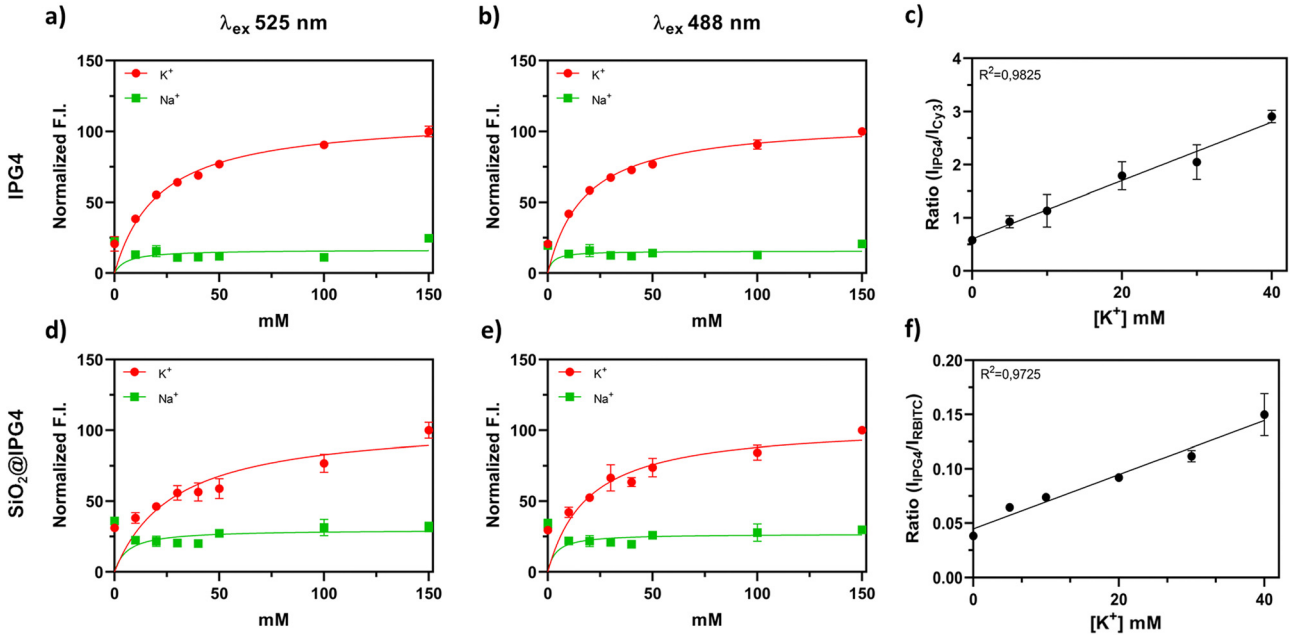

Fig. 2 Kinetic analyses of IPG4 in the presence of K^+ and Na^+ and ratiometric calibration curves of the developed microsensors. (a) Correlation between K^+ and Na^+ concentration and the fluorescence intensity of IPG4 dissolved in MES buffer, in the range of 0–150 mM (λ_{ex} 488 nm and λ_{ex} 525 nm, λ_{em} 545–650 nm); (b) correlation between K^+ and Na^+ concentration and the fluorescence intensity of IPG4 in the range of 0–150 mM (λ_{ex} 488 nm and λ_{ex} 525 nm, λ_{em} 545–650 nm); (c) ratiometric calibration of SiO_2@Cy3-IPG4 in the range of $[K^+]$ = 0–40 mM (λ_{ex} 488 nm, λ_{em} 545–650 nm); (d) correlation between K^+ and Na^+ concentration and the fluorescence intensity of SiO_2@IPG4 in the range of 0–150 mM (λ_{ex} 488 nm and λ_{ex} 525 nm, λ_{em} 545–650 nm); (e) correlation between K^+ and Na^+ concentration and the fluorescence intensity of SiO_2@IPG4 in the range of 0–150 mM (λ_{ex} 488 nm and λ_{ex} 525 nm, λ_{em} 545–650 nm); (f) ratiometric calibration of SiO_2@RBITC-IPG4 in the range of $[K^+]$ = 0–40 mM, with excitation (λ_{ex} 488 nm, λ_{em} 545–650 nm). All samples were dissolved or suspended in MES buffer (50 mM, pH 7.5). The analysis was performed using a CLARIO star plate reader in the spectral scan mode in a black 96 multiwell plate.

$[K^+]$ and fluorescence intensity. The enhanced fluorescence of IPG4 related to K^+ seemed to act as a quencher to A594 fluorescence intensity, with a sensitivity range between 0 and 40 mM, which is comparable with the properties of IPG4 (see Fig. S3, ESI†). However, despite the sensitivity of microparticles to K^+, they could not be used as ratiometric optical sensors due to the absence of a reference signal.

Only the microparticles carrying RBITC and Cy3 as reference dyes were suitable as ratiometric K^+ microsensors by spectrofluorimetric analyses, as shown in Fig. 2c and f. These two ratiometric microsensors showed sensitivity in the range of 0–40 mM K^+, in accordance with the results obtained with the free IPG4 probe.

Physicochemical characterization

The physicochemical properties of the three synthesized microparticles, namely SiO_2@IPG4, SiO_2@Cy3-IPG4 and SiO_2@RBITC-IPG4, were investigated by DLS.

As reported in Table 1, the microparticles had a hydrodynamic diameter between 1.5 and 2.0 μm, with a relatively low polydispersity index. As expected, the three systems showed a slightly negative surface charge due to the covalent bond of the negatively charged fluorophores. The size and morphology of the microsensors were also characterized by SEM analysis (Fig. 3). All of the three types of silica microparticles exhibited spherical shapes, with homogeneous smooth surfaces and good levels of monodispersity. The measured diameter of the SiO_2@IPG4 MPs, extracted from the SEM image analysis, was 1.374 ± 0.016 μm (Fig. 3a–c), which was comparable to the hydrodynamic diameter obtained by DLS analysis. The SiO_2@Cy3-IPG4 MPs appeared to be the most polydispersed sensors, with a mean diameter of 1.195 ± 0.039 μm (Fig. 3d–f). SiO_2@RBITC-IPG4 MPs were the smallest of the three systems, with a mean diameter of 1.171 ± 0.018 μm (Fig. 3g–i). Overall, a high level of reproducibility in the microparticle synthesis, with a size in the range of 1.0–1.5 μm, was achieved. The small fluctuations in the diameter and size distribution may be related to small differences in the reaction time and molecular weight of the dyes bound to the MP surface, which might affect the Stöber condensation, which is known to be highly sensitive to slight variations in the reaction conditions.[32]

Calibration of the ratiometric fluorescent K^+ sensing microparticles by CLSM imaging

The fluorescent ratiometric microsensors were calibrated by CLSM in MES buffers with a known concentration of K^+ in the range of 0 to 40 mM, as shown in Fig. 4. As shown in Fig. 4a and b, the SiO_2@RBITC-IPG4 microsensors displayed a linear response towards K^+ in the range of 0 to 30 mM, with an increase in the fluorescence intensity of the green channel. This lower sensitivity, compared to the fluorimetric calibration, might be related to different sensitivities of the CLSM, which

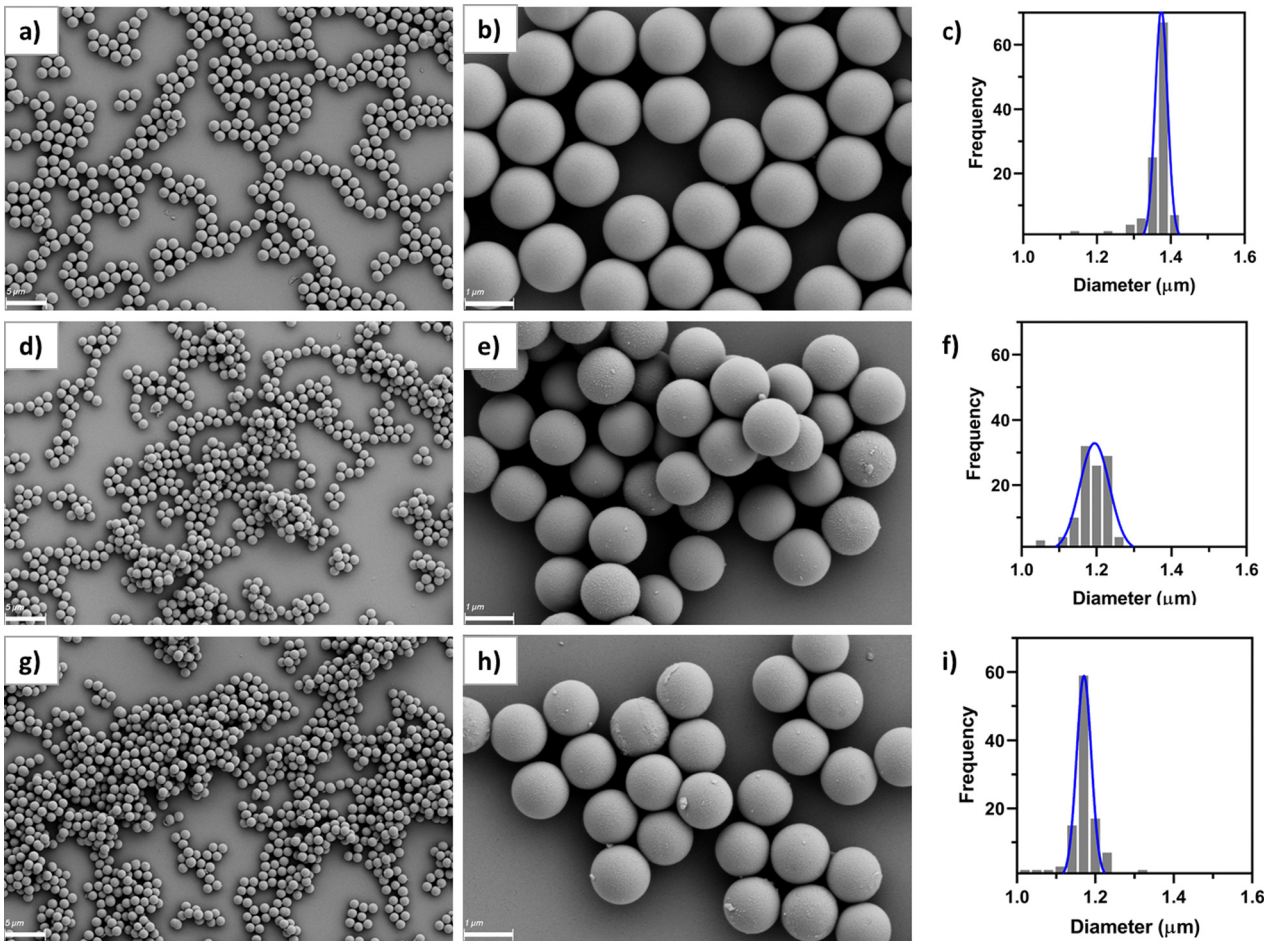

Fig. 3 Morphological characterization of K^+-sensors. SEM micrographs and size distribution of (a) SiO_2@IPG4 acquired at 5000× magnification; (b) SiO_2@IPG4 acquired at 30 000× magnification; (c) SiO_2@IPG4 size distribution chart based on SEM micrograph, mean diameter = 1.374 ± 0.016 μm; (d) SiO_2@Cy3-IPG4 acquired at 5000× magnification; (e) SiO_2@Cy3-IPG4 acquired at 30 000× magnification; (f) SiO_2@Cy3-IPG4 size distribution chart based on SEM micrograph, mean diameter = 1.195 ± 0.039 μm; (g) SiO_2@RBITC-IPG4 acquired at 5000× magnification; (h) SiO_2@RBITC-IPG4 acquired at 30000× magnification; (i) SiO_2@RBITC-IPG4 size distribution chart based on SEM micrograph, mean diameter = 1.171 ± 0.018 μm.

was confirmed by the LOD calculated for the two methods. The LOD obtained with spectrofluorimetric calibration is 1.7 mM, while the LOD for CLSM calibration is 9.51 mM. In contrast, calibration performed on the SiO_2@Cy3-IPG4 microsensors (see Fig. S4, ESI†) was not reproducible, as was SiO_2@RBITC-IPG4 (R^2 = 0.1953 and R^2 = 0.9736, respectively). In addition, despite being sensitive, the SiO_2@Cy3-IPG4 microparticles were not homogeneously functionalized and fluorescent (see Fig. S5, ESI†), with only a few particles displaying a fluorescence signal intense enough to allow for image analysis. These issues might be related to the lower quantum yield of Cy3 compared to RBITC and its different molecular structures, which might influence the synthesis of microsensors. The higher molecular weight, steric hindrance and negative charge of Cy3 may negatively affect the Stöber reaction involved in the synthesis of microparticles. Since SiO_2@RBITC-IPG4 MPs proved to be the best working system, we tested the stability of the microsensors over 7 days. In detail, the ratiometric SiO_2@RBITC-IPG4 MPs were incubated with different concentrations of K^+, and the emission peak of the sensing system was monitored over one week in order to record fluctuations occurring during storage. The results(Fig. S6, ESI†) indicated that the ratiometric signal of the MPs remained stable at each time point collected in the range of 0 to 40 mM [K^+]. Therefore, this evidence highlights the ability of the SiO_2@RBITC-IPG4 MPs to monitor its target analyte and supports the application of the optimized microparticles as a valuable and robust sensing tool for K^+ detection.

Biocompatibility evaluation

The biocompatibility of the ratiometric microsensors was assessed using an *in vitro* cell viability assay. We selected four different cell lines, three derived from different human tumor tissues in order to assess their toxicity in a broad spectrum of tumor models, and non-cancerous cell lines: breast cancer cells (MCF-7), human pancreatic adenocarcinoma cells (PANC-1), malignant melanoma cells (SK-MEL2) and murine fibroblasts (3T3). Cells were treated with three increasing concentrations (0.05–0.1–0.3 mg ml^{-1}) of K^+ sensing microparticles and their cytotoxic effects were evaluated by CellTiter-Glo® Cell Viability Assay. The graphs reported in Fig. 5b–d indicate the cell growth

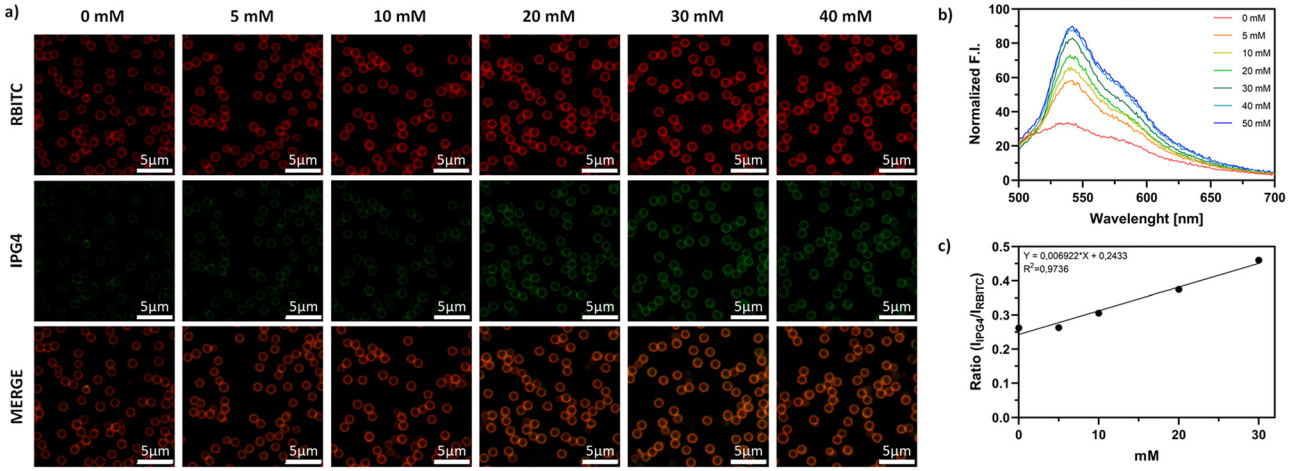

Fig. 4 Calibration of K^+-sensors. (a) Representative CLSM micrographs of SiO_2@RBITC-IPG4 microparticles incubated in MES buffer (50 mM) with adjusted concentrations of KCl (0, 5, 10, 20, 30, and 40 mM). RBITC red channel (λ_{ex} 555 nm, λ_{em} 600–700 nm), IPG4 green channel (λ_{ex} 488 nm, λ_{em} 500–600 nm), ZEISS LSM 700 objective 63×, zoom 2, scale bars, 5 µm; (b) emission spectra of SiO_2@RBITC-IPG4 microparticles incubated in MES buffer (50 mM) with adjusted concentrations of KCl (0, 5, 10, 20, 30, 40, 50 mM) with λ_{ex} 488 nm; and (c) calibration curve of SiO_2@RBITC-IPG4 based on CLSM image analysis, on the top of the plot with K^+ concentrations from 0 to 30 mM, standard error shown as SEM bar.

measurements derived from the luminescence signal that is proportional to the amount of ATP produced by metabolically active cells after incubation with CellTiter-Glo® reagent at 0, 24 and 48 hours of treatment. Treated cells showed little to no toxic effects due to the presence of microsensors. However, MCF-7 and SKMEL-2 cells reported a low toxic effect at the highest concentrations after 24 and 48 hours of treatment, but the cell growth percentage never reached values lower than 70%. These results suggest that SiO_2@RBITC-IPG4 microsensors are biocompatible and can be employed for sensing K^+ in *in vitro* cell culture systems.

Application of microsensors for live-cell K^+ detection

Potassium ions play different roles in biological processes, such as the regulation of cellular electrolyte metabolism, transport of nutrients and nerve transmission.[35] Moreover, dysregulated K^+ fluctuations are early signals of diseases, including electrolyte disorders, diabetes and cancer.[36] Therefore, the application of ratiometric optical microsensors in *in vitro* cell culture models could provide great benefits for monitoring cellular metabolism and responses to therapy under pathological conditions, such as cancer.

In this context, the capability of the SiO_2@RBITC-IPG4 microsensors to monitor variations in $[K^+]$ was tested in a 2D cell culture system of malignant melanoma, SKMEL-2. In order to induce K^+ efflux across the cell membrane, cells were stimulated with nigericin (1 µM for 1 hour), a K^+ ionophore that can form complexes with K^+, leading to a decrease in intracellular K^+ concentration.[37,38] CLSM acquisitions reported in Fig. 5a showed a decrease in the fluorescence intensity of the IPG4 dye in the unstimulated cells (CTRL), resulting in an orange overlay with the RBITC reference dye, indicating the physiological concentration of extracellular K^+. In contrast, in the treated condition, an increase in the fluorescence intensity of IPG4 was observed, indicating the efflux of intracellular K^+ from the cells. From image analyses, the K^+ concentration in the CTRL acquisition was determined to be 26 ± 0.25 mM. After 1 hour of nigericin treatment, the K^+ concentration in the extracellular environment increased up to 34 ± 0.25 mM. A comparative study based on fluorometric measurements of the cell culture supernatant collected from nigericin-treated or untreated cells and incubated with K^+ sensing microparticles is shown in Fig. S7 (ESI†). According to the fluorometric analysis, these data show an increase in K^+ concentration in the cell culture media collected from nigericin-treated cells compared to untreated cells. The K^+ concentration in the CTRL was determined as 5.12 ± 0.075 mM; on the contrary, after stimulus with nigericin, the K^+ concentration in the culture media increased up to 7.85 ± 0.06 mM. These results suggest that the SiO_2@RBITC-IPG4 microsensors are suitable for sensing K^+ with high spatial and temporal resolution in *in vitro* cell culture models.

Conclusions

The use of non-invasive tools for inorganic cation monitoring in biological samples is a widely explored field, and nanotechnology has led the way to new possibilities in terms of resolution and accuracy.

In this context, our microsensors offer a reliable tool for monitoring K^+ variations in the extracellular environment using imaging techniques and spectrofluorimetric analysis. Despite showing sensitivity in the millimolar range of K^+ concentrations, it is more appropriate to perform analyses in biological systems.

We designed, synthesized and characterized a ratiometric fluorescent microsensor that is suitable for the mapping of K^+ using high-resolution imaging techniques, such as CLSM. We chose silica as the starting material for our microsensor due to its inertness, biocompatibility, flexibility in synthesis and

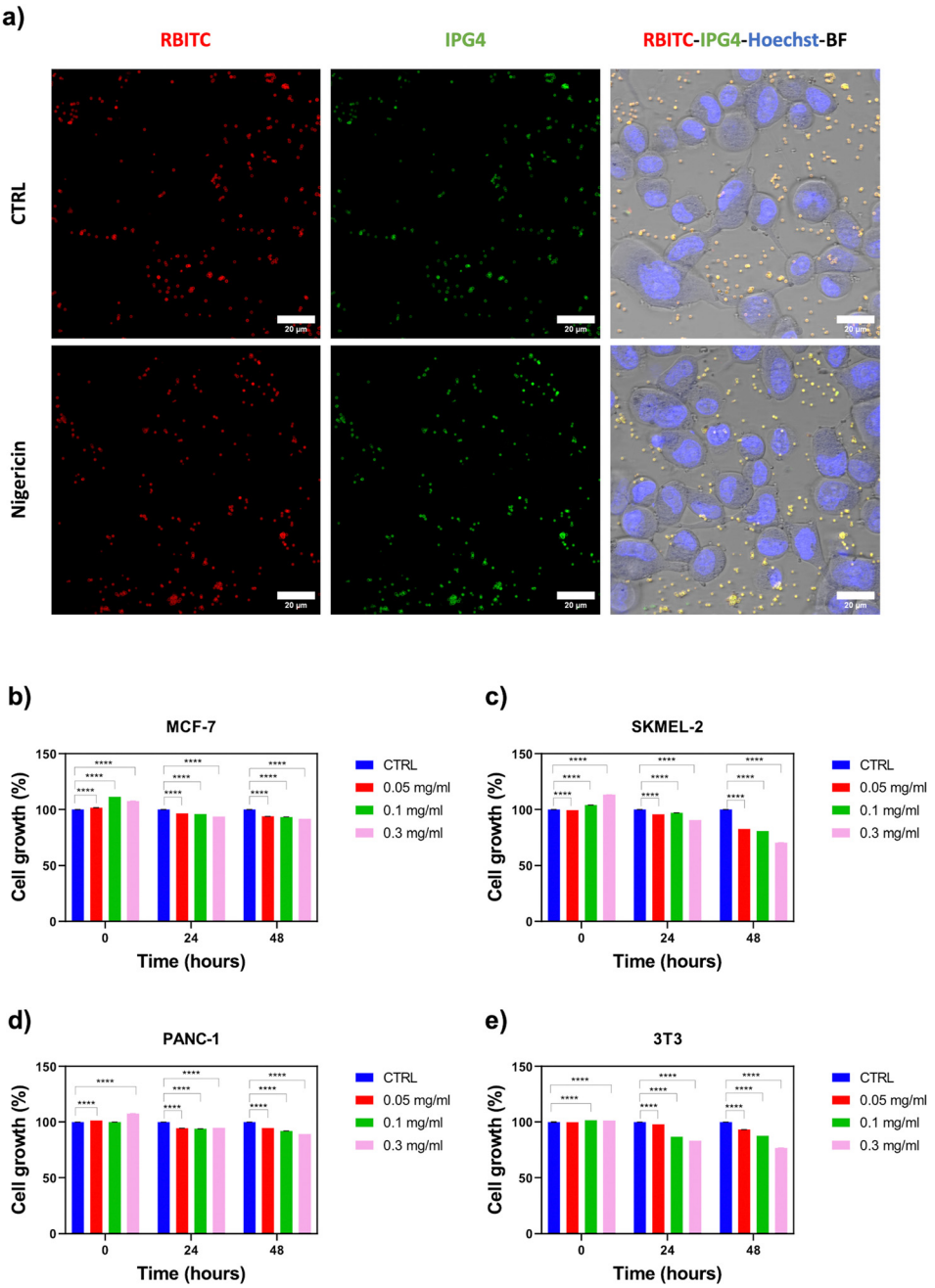

Fig. 5 Application of microsensors in biological systems: (a) CLSM micrographs showing microsensor properties after an induced pharmacological stimulus. SKMEL-2 cells were seeded in a 4-well chamber slide IBIDI and treated with nigericin at a concentration of 1 µM for 1 hour, and the fluorescence emission of the SiO_2@RBITC-IPG4 microparticles was recorded by CLSM. The RBITC red channel (λ_{ex} 555 nm, λ_{em} 600–700 nm), IPG4 green channel (λ_{ex} 488 nm, λ_{em} 500–600 nm), and Hoechst blue channel (λ_{ex} 405 nm, λ_{em} 415–500 nm). Image acquisitions were obtained with ZEISS LSM 980 (ZEISS, Germany), objective 40× Oil-immersion. The microsensor cytotoxicity was tested on (b) MCF-7, (c) SKMEL-2, (d) PANC-1 tumor cells and (e) 3T3 fibroblasts at three different concentrations (0.05–0.1–0.3 mg ml^{-1}) by CellTiter-Glo® Cell Viability Assay. The cell growth percentage was derived from the luminescence signal, which is proportional to the amount of ATP produced by metabolically active cells after incubation with CellTiter-Glo® reagent at 0, 24 and 48 hours of treatment. Values are the mean (±SE) of three independent experiments.

tailorability of the physical properties. We selected IPG4 as a K^+ sensitive probe because of its sensitivity and selectivity. We conjugated IPG4 to organically modified silica by amide bond formation without affecting its fluorescence and sensitivity. Notably, the binding of a reference dye required to produce ratiometric K^+ sensors, was critical for preserving the sensitivity of IPG4 to K^+ ions. The best result was obtained when IPG4 was coupled with rhodamine B isothiocyanate as the reference dye. The resulting fluorescent ratiometric microsensors displayed sensitivity in the range of 0 to 40 mM, which is optimal for extracellular tracking, considering that the interstitial K^+ concentration is always maintained in this range under

physiological conditions. Then, the biocompatibility of the K^+ sensors and their sensing properties were tested and confirmed in *in vitro* tumor cell culture models, which are suitable for use in extracellular K^+ detection. The developed sensing platform can be used to investigate the role of K^+ dysregulation in *in vitro* models of human diseases. A better understanding of how K^+ extracellular fluxes affect physiological processes might indeed help in the study of pathological conditions such as cancer, epilepsy and neuromuscular disorders. One challenge for *in vivo* imaging with the proposed sensor system is the emission of fluorescence in the visible light spectrum, which suffers from limited tissue penetration and potential interference from the autofluorescence of living cells. Therefore, while systemic administration in whole-animal or whole-organ tracking may not be suitable, this ratiometric K^+ sensor holds promise for application in skin monitoring. Dysregulation of potassium is a critical factor in skin responses to injury, particularly in wound healing processes. A notable example is skin burns, which are often associated with hyperkalemia. Given the well-documented biocompatibility of silica microparticles and further optimization of the sensor formulation, these microparticles could become a valuable tool for tracking potassium dynamics in the skin.

Data availability

The data supporting this article have been included as part of the ESI.†

Conflicts of interest

The authors declare no competing interests.

Acknowledgements

This work was supported by the European Research Council (ERC) under the European Union's Horizon 2020 Research and Innovation Program ERC Starting Grant ''INTERCELLMED'' (contract number 759959), the European Union's Horizon 2020 Research and Innovation Programme under grant agreement No. 953121 (FLAMIN-GO), the Associazione Italiana per la Ricerca contro il Cancro (AIRC) (MFAG-2019, contract number 22902), the ''Tecnopolo per la medicina di precisione'' (TecnoMed Puglia) - (Regione Puglia: DGR n.2117 of 21/11/2018, CUP: B84I18000540002), the Italian Ministry of Research (MUR) in the framework of the National Recovery and Resilience Plan (NRRP), ''NFFA-DI'' Grant (B53C22004310006), ''I-PHOQS'' Grant (B53C22001750006) and under the complementary actions to the NRRP, ''Fit4MedRob'' Grant (PNC0000007, B53C22006960001) funded by NextGenerationEU and the PRIN 2022 (2022CRFNCP_PE11_PRIN2022) funded by European Union – Next Generation EU.

References

1 H. R. Pohl, J. S. Wheeler and H. E. Murray, Interrelations between Essential Metal Ions and Human Diseases, 2013, pp. 29–47.
2 L. Kokoti, M. A.-M. Al-Karagholi and M. Ashina, *Curr. Pain Headache Rep.*, 2020, **24**, 1–8.
3 R. Köhling and J. Wolfart, *Cold Spring Harbor Perspect. Med.*, 2016, **6**, a022871.
4 R. Eil, S. K. Vodnala, D. Clever, C. A. Klebanoff, M. Sukumar, J. H. Pan, D. C. Palmer, A. Gros, T. N. Yamamoto, S. J. Patel, G. C. Guittard, Z. Yu, V. Carbonaro, K. Okkenhaug, D. S. Schrump, W. M. Linehan, R. Roychoudhuri and N. P. Restifo, *Nature*, 2016, **537**, 539–543.
5 X. Huang and L. Y. Jan, *J. Cell Biol.*, 2014, **206**, 151–162.
6 L. van de Velde, E. d'Angremont and W. Olthuis, *Talanta*, 2016, **160**, 56–65.
7 V. Georgiadis, A. Stephanou, P. A. Townsend and T. R. Jackson, *PLoS One*, 2015, **10**, e0129389.
8 K. Ertekin, M. Tepe, B. Yenigül, E. U. Akkaya and E. Henden, *Talanta*, 2002, **58**, 719–727.
9 M. Budiyanto, M. Yasin and M. A. Mahdiannur, *IOP Conference Series. Materials Science and Engineering*, IOP Publishing, 2021, p. 012004.
10 B. G. Kornreich, *J. Vet. Cardiol.*, 2007, **9**, 25–37.
11 A. Brüggemann, C. Farre, C. Haarmann, A. Haythornthwaite, M. Kreir, S. Stoelzle, M. George and N. Fertig, *Potassium Channels Methods Protoc.*, 2009, 165–176.
12 R. Rizzo, V. Onesto, S. Forciniti, A. Chandra, S. Prasad, H. Iuele, F. Colella, G. Gigli and L. L. Del Mercato, *Biosens. Bioelectron.*, 2022, **212**, 114401.
13 R. Rizzo, V. Onesto, G. Morello, H. Iuele, F. Scalera, S. Forciniti, G. Gigli, A. Polini, F. Gervaso and L. L. Del Mercato, *Mater. Today Bio*, 2023, **20**, 100655.
14 J. Krämer, R. Kang, L. M. Grimm, L. De Cola, P. Picchetti and F. Biedermann, *Chem. Rev.*, 2022, **122**, 3459–3636.
15 G. Grasso, F. Colella, S. Forciniti, V. Onesto, H. Iuele, A. C. Siciliano, F. Carnevali, A. Chandra, G. Gigli and L. L. del Mercato, *Nanoscale Adv.*, 2023, **5**, 4311–4336.
16 M. H. Lee, J. S. Kim and J. L. Sessler, *Chem. Soc. Rev.*, 2015, **44**, 4185–4191.
17 A. Chandra, S. Prasad, H. Iuele, F. Colella, R. Rizzo, E. D'Amone, G. Gigli and L. L. Del Mercato, *Chem. – Eur. J.*, 2021, **27**, 13318–13324.
18 G. Grasso, V. Onesto, S. Forciniti, E. D'Amone, F. Colella, L. Pierantoni, V. Famà, G. Gigli, R. L. Reis, J. M. Oliveira and L. L. del Mercato, *Bio-Des. Manuf.*, 2024, **7**, 292–306.
19 N. J. MacGilvary, Y. L. Kevorkian and S. Tan, *PLoS Pathog.*, 2019, **15**, e1007591.
20 X. Xie, G. A. Crespo, J. Zhai, I. Szilágyi and E. Bakker, *Chem. Commun.*, 2014, **50**, 4592–4595.
21 C. H. Lee, J. Folz, W. Zhang, J. Jo, J. W. Y. Tan, X. Wang and R. Kopelman, *Anal. Chem.*, 2017, **89**, 7943–7949.
22 L. L. Del Mercato, A. Z. Abbasi and W. J. Parak, *Small*, 2011, **7**, 351–363.
23 L. L. del Mercato, A. Z. Abbasi, M. Ochs and W. J. Parak, *ACS Nano*, 2011, **5**, 9668–9674.

24 J. Liu, L. Pan, C. Shang, B. Lu, R. Wu, Y. Feng, W. Chen, R. Zhang, J. Bu and Z. Xiong, *Sci. Adv.*, 2020, **6**, eaax9757.
25 M. A. Boyd, A. M. Davis, N. R. Chambers, P. Tran, A. Prindle and N. P. Kamat, *Cell. Mol. Bioeng.*, 2021, **14**, 459–469.
26 T. S. Rimmele and J.-Y. Chatton, *PLoS One*, 2014, **9**, e109243.
27 K. König, in *Methods Cell, Imaging*, ed. A. Periasamy, Springer, New York, NY, 2001, pp. 236–251.
28 ''IPG-4 AM,'' can be found under **https://ionbiosciences.com/product/ipg-4-am/**, n.d.
29 F. Meyer, *Signal Process.*, 1994, **38**, 113–125.
30 S. Ulrich, A. Osypova, G. Panzarasa, R. M. Rossi, N. Bruns and L. F. Boesel, *Macromol. Rapid Commun.*, 2019, **40**, 1900360.
31 H. Jaganathan and B. Godin, *Adv. Drug Delivery Rev.*, 2012, **64**, 1800–1819.
32 A. dos S. da Silva and J. H. Z. Dos Santos, *Adv. Colloid Interface Sci.*, 2023, 102888.
33 P. P. Ghimire and M. Jaroniec, *J. Colloid Interface Sci.*, 2021, **584**, 838–865.
34 C. Berney and G. Danuser, *Biophys. J.*, 2003, **84**, 3992–4010.
35 C. H. Lee, J. Folz, W. Zhang, J. Jo, J. W. Y. Tan, X. Wang and R. Kopelman, *Anal. Chem.*, 2017, **89**, 7943–7949.
36 U. K. Udensi and P. B. Tchounwou, *Int. J. Clin. Exp. Physiol.*, 2017, **4**, 111–122.
37 X. Zhou, F. Su, Y. Tian, C. Youngbull, R. H. Johnson and D. R. Meldrum, *J. Am. Chem. Soc.*, 2011, **133**, 18530–18533.
38 L. Rangasamy, V. Chelvam, A. K. Kanduluru, M. Srinivasarao, N. A. Bandara, F. You, E. A. Orellana, A. L. Kasinski and P. S. Low, *Bioconjugate Chem.*, 2018, **29**, 1047–1059.